

Note on the thermal stresses in passivated metal interconnects

P. Sharma,^{a)} H. Ardebili, and J. Loman

KWC1521, General Electric Corporate Research and Development, Niskayuna, New York 12309

(Received 29 May 2001; accepted for publication 27 July 2001)

An analytical model to compute thermal stresses in passivated metal interconnects is proposed in this article. Typical aspect ratio of passivated metal interconnects is 1 or less (frequently between 0.5 and 1). Previous Eshelby-based analytical model by Niwa *et al.* [J. Appl. Phys. **68**, 328 (1990)] is not very accurate as it fails to take into account the proximity of the interconnect to the free surface of the passivation. A recently proposed model by Wikström *et al.* [J. Appl. Phys. **86**, 6088 (1999)] precisely does not work when the aspect ratio < 1 . The analytical model proposed in this letter can predict stresses (average and spatial variations) in passivated metal interconnects with superior accuracy. The effect of free surface of passivation is fully taken into account and comparisons with previous works are presented. © 2001 American Institute of Physics. [DOI: 10.1063/1.1404124]

Thermal expansion mismatch is probably the leading cause of reliability issues in microelectronic devices.¹ Thermal stresses within metal interconnects lines etched on semiconductor surfaces can often cause reliability problems. An accurate determination of both average as well as gradients of internal stresses in metal interconnects is needed to make reliability predictions. As pointed out by Wikström *et al.*,² the finite element (FE) method can provide accurate solutions but is costly and time inefficient. Furthermore, it must be repeated for each change in material property and changes in geometrical parameters. Analytical models, which accomplish the same with reasonable accuracy, are therefore desirable.

An analytical model was presented by Niwa *et al.*³ based on Eshelby's equivalent inclusion concept.^{4,5} The metal interconnect lines were modeled as ellipsoidal cylindrical inclusion surrounded by an infinite amount of passivation. Clearly, their model is only likely to work if the distance of the interconnect line to free surface of passivation is large (so that they do not violate the implicit assumption in their model of an infinite amount of material surrounding the interconnect). This is generally not the case, as often the metal interconnect is nearly touching the free surface of the passivation or is very close to it. Recently, the work of Wikström *et al.*² caught the author's attention who have formulated their own analytical model and compared their results with detailed FE simulations and predictions from the Niwa³ Eshelby model. Their analytical model works very well in the limit when the aspect ratio (ratio of height to width) of the interconnect is very large. On the other hand it performs poorly when aspect ratio is < 1 . Since typically (due to processing limitations), aspect ratio of interconnect lines tend to be < 1 ; there is doubt about the use of Wikström *et al.*'s² analytical model for most practical situations. Eshelby's concept as used by Niwa *et al.*³ and later also by Korhonen *et al.*,⁶ can only be accurate when the interconnect is buried very deep in the passivation. It will be shown that the proposed analytical model is both qualitatively and quantitatively superior to that presented by Niwa *et al.*,³ especially

when the distance of the interconnect line is close to the free surface. In addition, the proposed model is superior to that of Wikström *et al.*² for aspect ratios < 1 .

The problem is sketched in Fig. 1. We seek to find the stress fields in the interconnect such that the effect of free surface of the passivation layer is also included. Like Niwa *et al.*³ we make use of Eshelby's equivalent inclusion concept. Eshelby's formalism is briefly reviewed here.^{4,5} Consider an infinite isotropic elastic matrix with an embedded inhomogeneity. An inclusion is defined as a region contained in a matrix with identical material properties but with a prescribed inelastic stress-free strain (commonly termed as eigenstrain).⁷ The eigenstrain has a finite value within the inclusion but is zero outside. Examples of some typical eigenstrains include thermal strains, phase change strains, etc. Let a pre-existing inelastic strain (eigenstrain), ϵ^p , exist in the inclusion. Then, the stress field within the interconnect can be represented as:^{4,5}

$$\sigma_{ij}^{\text{int}} = C_{ijkl}[\epsilon_{kl}^0 + S_{klmn}(\epsilon_{mn}^* + \epsilon_{mn}^p) - \epsilon_{kl}^* - \epsilon_{kl}^p]. \quad (1)$$

For an arbitrarily shaped inhomogeneity, \mathbf{S} is an integral operator on $(\epsilon^* + \epsilon^p)$. \mathbf{C} is the fourth-order elastic stiffness tensor for the matrix while \mathbf{C}^h is the fourth-order elastic stiffness tensor for the inhomogeneity, and ϵ^o is the far-field or overall strain. Conventional summation rules apply. Theo-

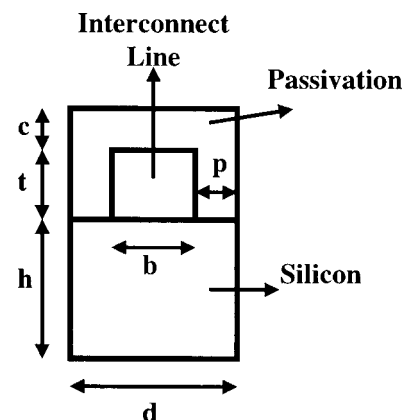


FIG. 1. Unit cell schematic of the problem.

^{a)}Electronic mail: sharma@crd.ge.com

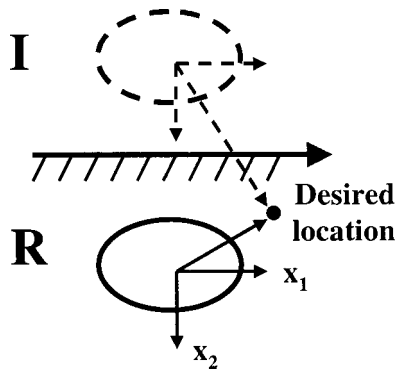


FIG. 2. Schematic of the solution.

retically, Eshelby's tensor can be derived for any shape, numerically, if not analytically. For some common shapes (e.g., ellipsoids), explicit analytical expressions can be derived based on the harmonic and biharmonic potentials of the inclusions (see, for example, Ref. 7). We will attempt to use Eshelby's concept for an inclusion located in *half-space*, in contrast to previous works^{2,3} which have used an infinite space solution. Some mathematical details of Eshelby's tensor are summarized later.

We model the current problem by a cylindrical inclusion in half-space located an arbitrary distance from the free edge. A schematic is shown in Fig. 2. For this problem, Eshelby's interior tensor becomes nonuniform.

As shown by Seo and Mura,⁸ stresses in the inclusion located close to the free surface can be computed using contributions from the mirror image (*I*) (with x_1 axis as the mirror) and the actual inclusion (*R*). Thus, the harmonic and biharmonic potentials are evaluated using both the image (*I*) and real (*R*) inclusion at the desired point. The harmonic and biharmonic potentials for this problem (necessary to evaluate Eshelby's tensor for half-space) can be derived using Green's function for semi-infinite elastic space. For the dilational eigenstrain problem, only the sum of the diagonal elements of Eshelby's tensor are needed and they are extracted from Seo and Mura⁸ and recorded at the end of the letter. The stresses can still be found by Eq. (1) although Eshelby's tensor is calculated from expressions given for half-space.

Numerical results are presented for the three diagonal stress components. Since we have a spatially variable solu-

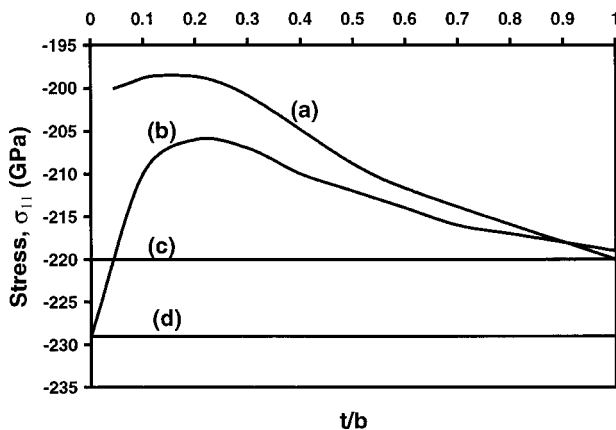


FIG. 3. Comparison of proposed model with previous works (σ_{11}) for $c/t = 0.5$; (a) (Ref. 2) FEM results, (b) proposed model, (c) (Ref. 2) analytical model, (d) Niwa (Ref. 1) Eshelby model.

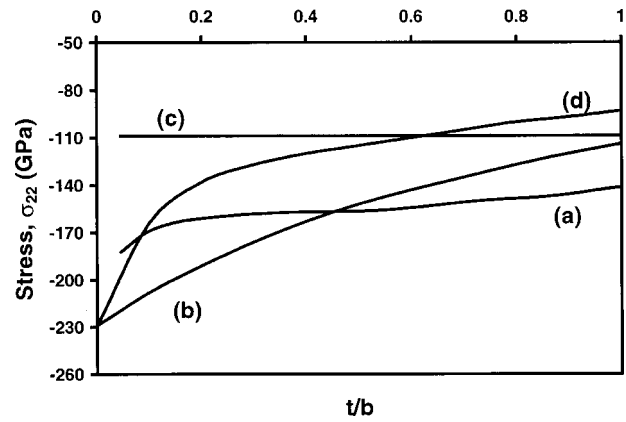


FIG. 4. Comparison of proposed model with previous works (σ_{22}) for $c/t = 0.5$; (a) Wikström (Ref. 2) FEM results, (b) proposed model, (c) Wikström (Ref. 2) analytical model, (d) Niwa (Ref. 3) Eshelby model.

tion, we calculate it at the center of the interconnect. The results are compared with the volume average stresses by the Ref. 3. Eshelby model. For their case, volume average stress is the same as stress at the center since their results are uniform within the inclusion. We also compare our results with the Ref. 2 analytical model and FE results. Figures 3–5 compare the diagonal stress components, respectively, σ_{11} , σ_{22} , σ_{33} . Note that the FE results and analytical model results of Ref. 2 were extracted from the plots as actual numbers were not available, however, the Ref. 3 Eshelby based model was implemented independently by the present authors.

As seen from Fig. 3, our model qualitatively behaves very similar to the finite element result and is superior to both previous works.^{2,3} Figures 3–5 clearly indicate that both the qualitative and quantitative behavior of our solution is better than the Refs. 2 and 3 analytical model. Our results are closer to the FE solution. The results are presented for the case $c/t=0.5$, $b=1.5 \mu\text{m}$ (same as in Ref. 2). The material properties used are the same. For cases other than $c/t=0.5$, i.e., $c/t=0$ (when interconnect is touching the free surface), a direct comparison with the results of Wikström *et al.*² is not possible as they have couched their results in ratios and are not in a convenient form for comparison. However, our results for the case $c/t=0$ are compared with the Ref. 3 Eshelby based model. For the case of $c/t=0$, all stress com-

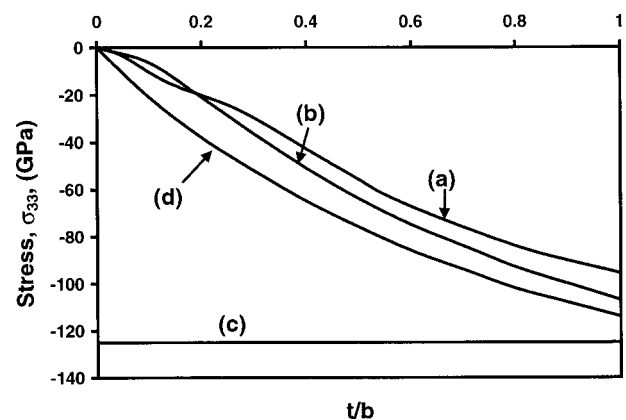


FIG. 5. Comparison of proposed model with previous work (σ_{33}) for $c/t = 0.5$; (a) Wikström (Ref. 2) FEM results, (b) proposed model, (c) Wikström (Ref. 2) analytical model, (d) Niwa (Ref. 3) Eshelby model.

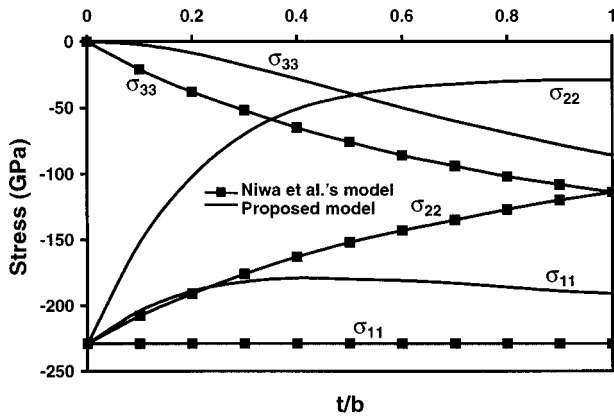


FIG. 6. Comparison with Niwa (Ref. 3) Eshelby model for $c/t=0$.

ponents are plotted together and are shown in Fig. 6. This is the case where the model of Ref. 3 is likely to perform poorly due to the implicit assumption in the model of infinite material surrounding the interconnect. We have verified the validity of our numerical results for half-space by comparing with numerical results of Seo and Mura.⁸

In summary, an improved analytical model to compute the thermal stresses and their gradients in passivated metal interconnects was presented. Results compare well with existing work. In particular, this model is superior for aspect ratios less than one (as is typical) and for the case when the top surface of interconnect is very close to the free surface of the passivation layer (as also typical). Furthermore, unlike previous analytical models, ours can provide stress gradients and as shown previously³ inclusion of plastic relaxation is also straightforward when using Eshelby's approach.

Mathematical details of Eshelby's tensor: Eshelby^{4,5,7} showed that the disturbed strain field due to the eigenstrain is given by

$$\varepsilon_{ij}(\mathbf{x}) = \frac{1}{8\pi(1-\nu)} [\Psi_{kl,klj} - 2\nu\Phi_{kk,ij} - 2(1-\nu) \times (\Phi_{ik,kj} + \Phi_{jk,ki})], \quad (2)$$

where, Ψ and Φ are biharmonic and harmonic potentials of the ellipsoid. They are given as

$$\Psi_{ij}(\mathbf{x}) = \int_{\Omega} |\mathbf{x}-\mathbf{x}'| \varepsilon_{ij}^*(\mathbf{x}') d\mathbf{x}',$$

$$\Phi_{ij}(\mathbf{x}) = \int_{\Omega} \frac{1}{|\mathbf{x}-\mathbf{x}'|} \varepsilon_{ij}^*(\mathbf{x}') d\mathbf{x}'. \quad (3)$$

Eshelby⁴ showed that for ellipsoids with uniform eigenstrains, Eq. (2) can be reduced to (in the interior of the inclusion):

$$\varepsilon_{ij} = S_{ijkl} \varepsilon_{kl}^*. \quad (4)$$

Here, S_{ijkl} is called Eshelby's tensor (and is uniform for ellipsoids) and can be evaluated explicitly by integrating the harmonic and biharmonic potentials. The components of this tensor are available in closed form and have been recorded by Eshelby^{4,5} and Mura.⁷ Eshelby's exterior S_{ijkl} is given by:⁵

$$S_{ijkl} = \frac{1}{8\pi(1-\nu)} [\Psi_{,klj} - 2\nu\delta_{kl}\Phi_{,ij} - (1-\nu)(\Phi_{,kj}\delta_{il} + \Phi_{,ki}\delta_{jl} + \Phi_{,lj}\delta_{ik} + \Phi_{,li}\delta_{jk})], \quad (5)$$

where Eshelby's tensor for full space is obtained by using Eq. (5).

The necessary Eshelby's tensor components for dilatational eigenstrain for half-space problem: The following notation is used: Superscript I represents the image while R represents the real inclusion. The harmonic potentials and the derivatives are the same as used previously but the form of Eshelby's tensor is different than Eq. (5). Only dilatational eigenstrain is considered here. For the dilatational problem, only the following sums of the Eshelby's tensors are needed and can be easily extracted from Seo and Mura⁸

$$S_{1111} + S_{1122} + S_{1133} = \frac{-(1+\nu)}{4\pi(1-\nu)} [\Phi_{,11}^R + (3-4\nu)\Phi_{,11}^I + 2x_3\Phi_{,311}^I],$$

$$S_{2211} + S_{2222} + S_{2233} = \frac{-(1+\nu)}{4\pi(1-\nu)} [\Phi_{,22}^R + (3-4\nu)\Phi_{,22}^I + 2x_3\Phi_{,322}^I], \quad (6)$$

$$S_{3311} + S_{3322} + S_{3333} = \frac{-(1+\nu)}{4\pi(1-\nu)} [\Phi_{,33}^R - (3-4\nu)\Phi_{,33}^I + 2x_3\Phi_{,333}^I + 2\Phi_{,33}^I].$$

Support from General Electric Corporate Research and Development is gratefully acknowledged. Helpful discussions with Professor Abhijit Dasgupta are also acknowledged.

¹ *Plastic Encapsulated Microelectronics*, edited by M. Pecht, L. T. Nguyen, and E. B. Hakim (Wiley, New York, 1995).

² A. Wikström, P. Gudmundson, and S. Suresh, *J. Appl. Phys.* **86**, 6088 (1999).

³ H. Niwa, H. Yagi, H. Tsuchikawa, and M. Kato, *J. Appl. Phys.* **68**, 328 (1990).

⁴ J. D. Eshelby, *Proc. R. Soc. London, Ser. A* **241**, 376 (1957).

⁵ J. D. Eshelby, *Proc. R. Soc. London, Ser. A* **252**, 561 (1959).

⁶ M. A. Korhonen, R. D. Black, and C. Y. Li, *J. Appl. Phys.* **69**, 1748 (1991).

⁷ T. Mura, *Micro-Mechanics of Defects of Solids* (Martinus Nijhoff, Hague, 1987).

⁸ K. Seo and T. Mura, *J. Appl. Mech.* **46**, 568 (1979).